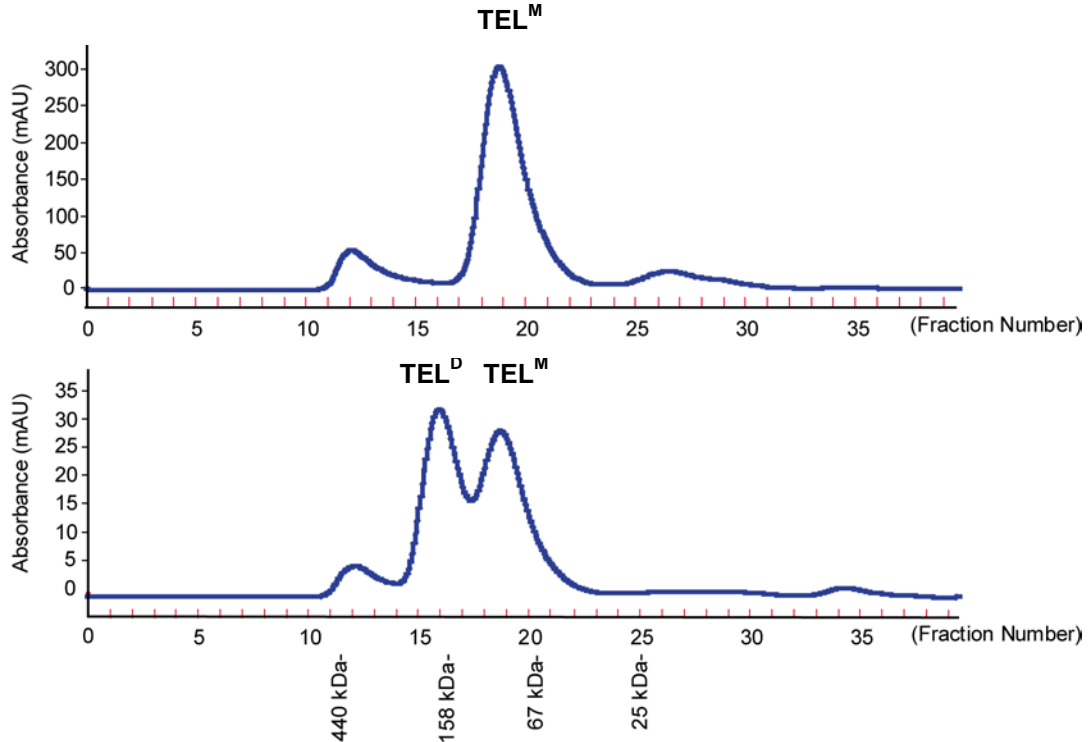


## SUPPLEMENTAL MATERIAL

### DNA BINDING BY THE ETS PROTEIN TEL(ETV6) IS REGULATED BY AUTOINHIBITION AND SELF-ASSOCIATION

Sean M. Green, H. Jerome Coyne III, Lawrence P. McIntosh, Barbara J. Graves

#### Supplemental Figure S1



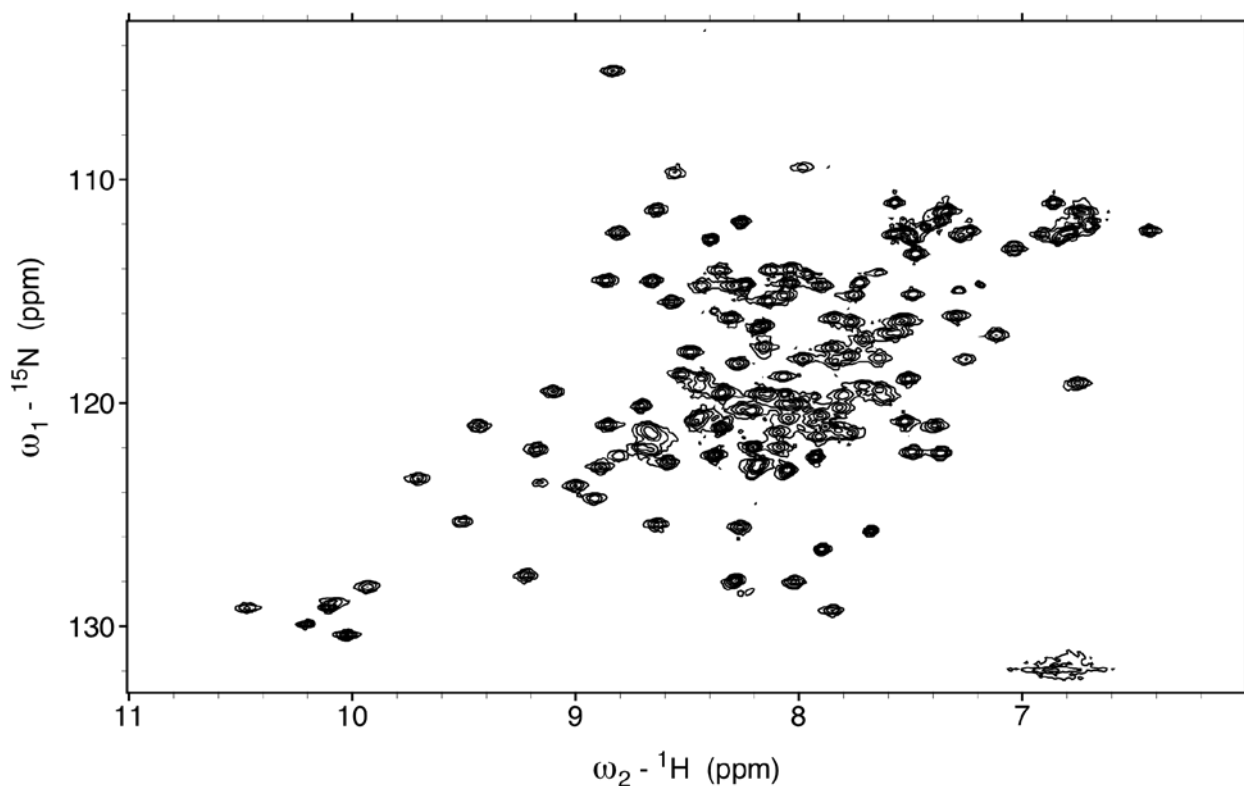
Full length TEL exhibits the self-association properties of the isolated PNT domain of TEL. A single point mutation in either of these surfaces (A94D or V113E) was sufficient for disrupting self-association. However, each of these mutants retains one of the native surfaces involved in polymerization, such that a mixture of the mutants yields a heterodimer (Fig. 1; Kim, C. A., Phillips, M. L., Kim, W., Gingery, M., Tran, H. H., Robinson, M. A., Faham, S., and Bowie, J. U. (2001) *EMBO J.* **20**, 4173-4182).

Gel filtration chromatography on a Superdex 75 column was used to monitor dimer formation of full length TEL (20 mM Na-citrate pH 5.3, 150 mM KCl, 1 mM EDTA, 1 mM DTT, 0.2 mM PMSF, and 10% glycerol). Position of molecular mass markers (indicated) were established by chromatography under identical conditions. First, full length  $TEL^M$ , with the two mutations A94D and V113E was chromatographed ( $\sim 200 \mu\text{M}$ ) to monitor the elution profile of TEL monomers (upper panel).  $TEL^M$  eluted with an apparent molecular mass of  $\sim 100$  kDa. Although the molecular mass of  $TEL^M$  is  $\sim 56$  kDa, an explanation for this discrepancy is discussed below. To monitor dimerization, recombinant mutants with either the A94D or V113E substitutions were mixed at a 3:1 molar ratio (30  $\mu\text{M}$ , A94D and 10  $\mu\text{M}$ , V113E), equilibrated at  $4^\circ\text{C}$  for one hr, then chromatographed (lower panel). We propose the first peak contains TEL dimers due to its elution at double the apparent molecular mass of  $TEL^M$  control peak

(upper panel), whereas the second peak contains TEL<sup>M</sup>. Because the isolated PNT domain self-associates with a  $K_d \sim 2$  nM, the protein concentrations used in this experiment should yield stoichiometric dimer formation (i.e. 1:2 ratio of dimer to A94D monomer). Indeed, the two peaks are nearly equivalent in absorbance, suggesting complete dimer formation. The small peak that elutes near 440KDa marker in observed in both chromatographs is not protein.

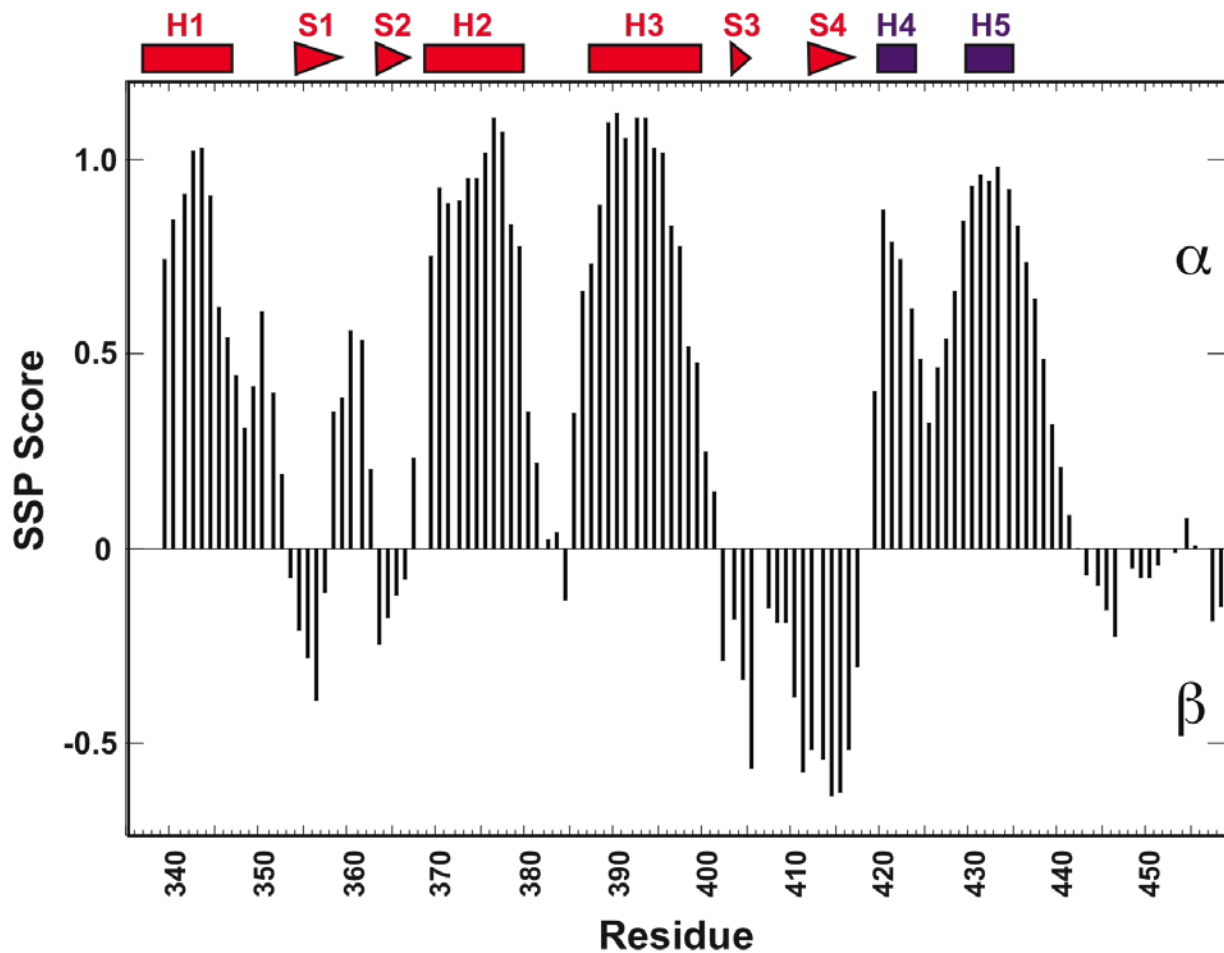
TEL<sup>M</sup> displays a retention time that suggests a mass of  $\sim 100$  kDa, whereas the molecular mass of TEL<sup>M</sup> is  $\sim 56$  kDa. Because separation by gel filtration is strongly dependent on the Stoke's radius of the protein, discrepancies in molecular mass are commonly observed for proteins that contain unstructured regions or non-globular shapes. Based on experiments reported here, we propose that TEL contains two globular domains separated by a flexible region. Therefore, such deviation in the apparent molecular mass of TEL might be expected.

### Supplemental Figure S2



The <sup>15</sup>N-HSQC spectrum of uniformly <sup>15</sup>N/<sup>13</sup>C-labeled TEL(ΔN335:ΔC458) confirms that the deletion fragment adopts a well-ordered structure in solution. The protein was expressed in *E. coli* BL21 (λDE3) cells grown in <sup>15</sup>N/<sup>13</sup>C-enriched M9 media using a pET28b vector encoding residues R335-R458 of TEL preceded by a His<sub>6</sub>-tag and a thrombin cleavage site. The protein was purified by Ni<sup>+2</sup> affinity chromatography, followed by thrombin treatment (leaving an N-terminal Gly-Ser-His-Met sequence). The final sample was 0.2 mM protein in a pH 5.8 buffer consisting of 50 mM phosphate and 50 mM NaCl. The main chain <sup>1</sup>H, <sup>13</sup>C, and <sup>15</sup>N signals of TEL(ΔN335:ΔC458) were assigned using standard multidimensional heteronuclear correlation spectra recorded with Varian Unity 500 and Inova 600 spectrometers (not shown).

### Supplemental Figure S3



Identification of the secondary structural elements of TEL( $\Delta$ N335: $\Delta$ C458) using the Secondary Structure Propensity (SSP) algorithm (Marsh, J.A., Singh, V.K., Jia, Z., Forman-Kay, J.D. (2006) *Protein Sci.* **15**, 2795-2804). SSP scores, calculated from  $^{13}\text{C}^\alpha$ ,  $^{13}\text{C}^\beta$ ,  $^1\text{H}^\alpha$ , and  $^{13}\text{C}'$  chemical shifts, approach +1 and -1 with increasing  $\alpha$ -helical and  $\beta$ -strand, respectively. The ETS domain is composed of 3 helices (H1-H3) on a 4-stranded  $\beta$ -sheet scaffold (S1-S4). The CID contains 2 additional helices (H4 and H5). This is consistent with the unpublished structure of the TEL( $\Delta$ N334: $\Delta$ C456) fragment deposited in the Protein Data Bank (2DAO.pdb), albeit suggestive of longer helices H4 and H5. The upper cartoon depicts the helices (rectangles) and strands (triangles) identified in 2DAO.pdb using the Promotif algorithm (Hutchinson, E.G., Thornton, J.M. (1996) *Protein Sci.* **5**, 212-220).

**Supplemental Table 1**  
**Primers and Templates used for cloning of TEL species**

NdeI and KpnI restriction sites are underlined in the N- and C-terminal primers, respectively. To fully replicate the structurally-defined fragment  $\Delta$ N334: $\Delta$ C436 species were designed to retain non-TEL sequences (bold). Sites of directed mutagenesis are indicated (underlined italic).

Construct	Template	N-terminal Primer	C-terminal Primer
$\Delta$ C436 (A94D;V113E)	pET28b- TEL(A94D;V113E)	5' <u>GCAGCC</u> CATATGT CTGAGACTCC 3'	5'CGGCATGGTACCCTATCCAG <b>AAGAGGGTCCAGACAGCTCT</b> TGAGACTCGAGGTGTTC 3'
$\Delta$ C426 (A94D)	pET28b-TEL(A94D)	same as $\Delta$ C436 (A94D;V113E)	5'CGGCGGGGTACCCTACCGGC CACTCATGATCTCATCTGGG 3'
$\Delta$ C426 (V113E)	pET28b-TEL(V113E)	same as $\Delta$ C436 (A94D;V113E)	same as $\Delta$ C426 (A94D)
$\Delta$ C426 (A94D;V113E)	same as $\Delta$ C436(A94D;V113E)	same as $\Delta$ C436 (A94D;V113E)	same as $\Delta$ C426 (A94D)
$\Delta$ N127	same as $\Delta$ C436(A94D;V113E)	5' AAGCAG <u>CATATG</u> TCTCGAATGCTCTT CTCACC 3'	5'CGGCGGGGTACCCTATTCCC GGGTCTCTTC 3'
$\Delta$ N331	same as $\Delta$ C436(A94D;V113E)	5'GCCCATTCATAT <u>GATAGCAGACTGT</u> AGACTGC 3'	same as $\Delta$ N127
$\Delta$ N331: $\Delta$ C426	same as $\Delta$ C436(A94D;V113E)	same as $\Delta$ N331	same as $\Delta$ C426 (A94D)
$\Delta$ N334: $\Delta$ C436	same as $\Delta$ C436(A94D;V113E)	5'GCCCATTCATAT <u>GGGATCTTCTGG</u> <b>ATCTTCTGGATGT</b> AGACTGCTTTGGG AT 3'	same as $\Delta$ C436(A94D;V113E)
$\Delta$ N334: $\Delta$ C436 (E431A)	same as $\Delta$ C436(A94D;V113E)	same as $\Delta$ N334: $\Delta$ C436	5'CGGCATGGTACCCTATCCAG <b>AAGAGGGTCCAGACAGCTCT</b> <b>TGAGACTCGAGGTGGGCTAGA</b> CGGTCTGT 3'
$\Delta$ N334: $\Delta$ C434 (E434A)	same as $\Delta$ C436(A94D;V113E)	same as $\Delta$ N334: $\Delta$ C436	5'CGGCATGGTACCCTATCCAG <b>AAGAGGGTCCAGACAGCTCT</b> <b>TGAGAGGC</b> GAGGTGTTC 3'
$\Delta$ N334: $\Delta$ C434 (E431A;E434A)	same as $\Delta$ C436(A94D;V113E)	same as $\Delta$ N334: $\Delta$ C436	5'CGGCATGGTACCCTATCCAG <b>AAGAGGGTCCAGACAGCTCT</b> <b>TGAGAGGC</b> GAGGTGGGCTAGA CGGTCTGT 3'

**Supplemental Table 2****Oligonucleotides used to create DNA duplexes for testing determinants of dimer binding.**

ETS binding sites are indicated (underlined). The spacing between binding sites was defined as one helical turn = 10.8 bp. Complementary oligonucleotides (not shown) were designed such that upon annealing, 5' and 3' overhangs were generated to mimic cleavage by PstI and KpnI, respectively.

Binding Site	Top strand
5 helical turns (54 bp)	5'GCTGG <u>CCGGAAGT</u> TGTTACTGTAGCAACTGTTGTGTAGTGTATGTATTT GCGTAGTATGCTTACTGTACTAGCATTAGCTTA ATGCTAACGGTAC 3'
6 helical turns (65 bp)	5'GCTGTGTTAAGTGTGG <u>CCGGAAGT</u> CAACTGTTGTGTAGTGTATGTATTT GCGTAGTATGCTTACTGTACTAGCATTAGCTTA GCTTAATGCTAACGGTAC 3'
7 helical turns (76 bp)	5'GCTGTGTTAAGTGTGTTACTGTAGCAG <u>CCGGAAGT</u> TAGTGTATGTATTT GCGTAGTATGCTTACTGTACTAGCATTAGCTTA GCTTAATGCTAACGGTAC 3'
10 helical turns (108 bp)	5'GCTGTGTTAAGTGTGTTACTGTAGCAACTGTTGTGTAGTGTATGTATTT GCGTAGTATG <u>CCGGAAGT</u> ACTAGCATTAGCTTA GCTTAATGCTAACGGTAC 3'